Opposing modulation of Cx26 gap junctions and hemichannels by CO_2

Sarbjit Nijjar[1], Daniel Maddison[1], Louise Meigh[1], Elizabeth de Wolf[1], Thomas Rodgers[2], Martin Cann[3], Nicholas Dale[1]

[1]School of Life Sciences
University of Warwick
Coventry
CV4 7AL

[2]School of Chemical Engineering and Analytical Science
University of Manchester
Oxford Road
Manchester
M13 9PL

[3]Department of Biosciences
Durham University
Stockton Road
Durham
DH1 3LE

Abstract

Cx26 hemichannels are opened by modest levels of CO_2 (PCO_2 55 mmHg) acting via a novel carbamylation mechanism to bias the hemichannel to the open state. In the hemichannel, CO_2 non-enzymatically carbamylates Lys125, and the resulting carbamate forms a salt bridge to Arg104 of the neighbouring subunit. By contrast, similar modest levels of CO_2 cause Cx26 gap junction closure. Gap junctions of Cx31, a beta connexin that lacks the carbamylation motif, are insensitive to these levels of CO_2. Mutations of the carbamylation motif, Lys125Arg and Arg104Ala, which abrogate hemichannel opening in Cx26, also prevent gap junction closing. Elastic network modelling suggests that the lowest entropy state, when CO_2 is bound, is in the open configuration for the hemichannel and the closed configuration for the gap junction Surprisingly, we conclude that the opposing actions of CO_2 on Cx26 gap junctions and hemichannels results from carbamylation of the same residues.

Introduction

The canonical function of connexins is to form intercellular junctions between cells –gap junctions – through the docking of hexameric connexons in the opposing membrane of each cell. However, the individual connexons –known as hemichannels –can also function on their own (Stout et al., 2004; Weissman et al., 2004; Pearson et al., 2005; Huckstepp et al., 2010b). Hemichannels act as plasma membrane channels, which in addition to mediating transmembrane ionic currents, also permit the transmembrane fluxes of small molecules such as ATP (Stout et al., 2002; Pearson et al., 2005; Kang et al., 2008; Huckstepp et al., 2010a).

We have studied the hemichannels of connexin26 (Cx26) and found that these hemichannels are directly gated by CO_2 (Huckstepp et al., 2010a; Meigh et al., 2013; Meigh et al., 2014). CO_2 opens the hemichannel and permits the efflux of ATP, which can act as a neurotransmitter. This is particularly important in the CO_2 sensitive control of breathing, where Cx26 hemichannels in the medulla oblongata act as novel chemosensory transducers (Huckstepp et al., 2010a; Huckstepp and Dale, 2011). The action of CO_2 on Cx26 occurs via carbamylation of the residue K125. The carbamylated lysine forms a salt bridge to R104 of the neighbouring subunit. These intersubunit carbamate bridges lock the hemichannel in the open configuration (Meigh et al., 2013).

Although the actions of CO_2 on Cx26 hemichannels are well characterized, we have not studied the action of CO_2 on Cx26 gap junctions. When the two connexons dock to form a complete gap junction, there is likely to be significant conformational rearrangement and constraint of the resulting dodecameric complex. Therefore, we cannot assume that CO_2 will modulate a complete gap junction in the same way as a hemichannel. In this paper, we report the actions of CO_2 on gap junctions

formed between pairs of HeLa cells expressing Cx26. To our surprise we find that modest increases in CO_2 *close* complete gap junctions, and that this is most likely a direct effect mediated through its binding to the same residues that result in the *opening* of the hemichannel. This result reinforces the need to develop further high-resolution structures for Cx26 hemichannels and gap junctions with and without CO_2 bound.

Results

Our extensive prior studies on the parental HeLa cells show them to be devoid of Cx26, and of any other type of hemichannel. Furthermore, the parental HeLa cells exhibit no sensitivity to CO_2 in a variety of assays to probe hemichannel function.

To study gap junctions, we made simultaneous whole cell recordings from isolated pairs of Cx26-expressing HeLa cells that were in close contact. These cells had a high probability of being electrically coupled. On establishing whole cell recordings from each cell, the cells were clamped at a holding potential of -50 mV. We used a simple protocol of repeated 10 mV steps, alternating in each cell, to measure both the whole cell conductance of each cell and the junctional conductance between the cells (Figure 1). In all the illustrations, the outward currents during the voltage steps are a measure of the whole cell conductance, and the inward currents during the voltage steps are proportional to the junctional conductance.

Cx26 Gap junctions are closed by CO_2

After establishing stable recordings, we switched the extracellular medium from control saline (PCO_2 35 mmHg), to a hypercapnic saline (PCO_2 55 mmHg) at a constant extracellular pH of 7.5. In every case we found that the CO_2 stimulus caused a reduction of junctional coupling (Figure 2). In some cases, this was a partial effect and, in other cases, the Cx26 gap junctions were completely closed. Overall the median change of the Cx26 gap junction conductance (from control to CO_2 stimulus) was -5.6 nS (95% confidence limits -11.9 and -3.2 nS, n=29).

We also observed that the effect of CO_2 was sometimes reversible (16/29 cases), and on other occasions irreversible within the duration of the whole cell recordings (13/29 cases, Figure 2, Figure 2, Supplement 1). After washout of CO_2, and failure to reverse the reduction of the junctional conductance, the remaining junctional conductance was insensitive to further application of CO_2 (Figure 2, Supplement 1). Gap junctions were occasionally observed between untransfected parental HeLa cells, but these displayed no sensitivity to CO_2 (Figure 5a).

We measured both the whole cell conductance and the junctional conductance. As the junctional conductance was reduced by CO_2, we would also expect the whole cell conductance to reduce simultaneously, as the gap junction represents a current path out of the cell. We did indeed observe parallel reductions of the whole cell and junctional conductances (Figure 2). However, in some cases the whole cell conductance did not reduce appreciably despite a reduction in the junctional conductance, suggesting that a parallel increase in whole cell conductance may have masked the expected reduction. This is most easily explained if the pairs of HeLa cells express both Cx26 hemichannels and gap junctions -the simultaneous opening of Cx26 hemichannels and closure of gap junctions would mask any reductions of net whole cell conductance. Indeed, in some cases (particularly in cells that had not been *in vitro* for more than one day) we saw simultaneously both an increase in whole cell conductance, and a loss of gap junction coupling (Figure 2, Supplement 2). Interestingly, the CO_2-dependent opening of the hemichannels was readily reversible, yet in the same cells the CO_2-dependent closure of the gap junction did not reverse, suggesting a fundamental difference in the kinetics of modulation of hemichannels and gap junctions by CO_2 (Figure 2, Supplement 2).

Our results lead to the surprising conclusion that CO_2 has opposite effects on Cx26 gap junctions and hemichannels. Not only does CO_2 close the gap junctions in contrast to opening the hemichannels, this closure of the gap junction appears to be less reversible, at least in some cases, than the modulation of the hemichannel.

Permeability to fluorescent dyes shows CO_2-dependence

To verify our patch clamp results by a different method, we studied CO_2-sensitivity of the permeation of a fluorescent glucose analogue (2-Deoxy-2-[(7-nitro-2,1,3-benzoxadiazol-4-yl)amino]-D-glucose, NBDG) through the gap junctions (Figure 3a). NBDG could readily permeate Cx26 gap junctions, but not the hemichannels (Figure 3, supplement 1). Whole cell recordings were made from a single cell in a coupled pair or group. The patch electrode contained NBDG, and we measured the time it took for the dye to diffuse into a coupled cell and achieve 10% of the fluorescence intensity of the donor cell. We performed this assay under two conditions -starting in solutions with a PCO_2 of 35 mmHg, and then in cells where the PCO_2 started at 55 mmHg and was then swapped after 2 minutes to a PCO_2 of 35 mmHg. In cells that started with a low PCO_2 the NBDG permeated into the coupled cells rapidly (Figure 3 b,c). However, when the recording was initiated in saline with a PCO_2 of 55 mmHg, there was little permeation during the period of high PCO_2 and this only occurred once the PCO_2 was reduced to 35 mmHg. As a result, the time taken for the fluorescence to reach 10% of the donor cell was much longer than when the recordings were initiated in low PCO_2 (Figure 3c).

CO_2 acts directly on the gap junction

A reduction of pH is well known to close gap junctions. It is possible therefore that the closing effect of CO_2 on the Cx26 gap junction is mediated by a reduction of intracellular pH. Our CO_2 stimulus is "isohydric" -delivered at constant extracellular pH by reason of a simultaneous increase in extracellular HCO_3^-. Under these conditions, although CO_2 will enter the cell and cause acidification, the corrective extrusion of acid by the cell (mediated in large part by transporter mediated influx of HCO_3^-) is enhanced, and any resulting acidification is only transient. As the closure of the gap junction was not transient, this hypothesis seemed unlikely. Nevertheless, we tested whether CO_2 might act to close the gap junction via the same residues that are involved in hemichannel opening.

Cx31 is closely related to Cx26, however it lacks the carbamylation motif and its hemichannels are insensitive to CO_2 (Meigh et al., 2013). We made recordings from pairs of Cx31 expressing HeLa cells and found that neither the whole cell conductance, nor the gap junction conductance were altered by application of hypercapnic saline (Figure 4, 5a; change in conductance 0.07 nS, 95% confidence limits 0.44 and -0.29 nS, n=12). Given the close homology of Cx31 and Cx26, this suggests that any intracellular pH changes resulting from the application of hypercapnic saline are insufficient to alter the gap junction conductance.

The carbamylation of Lys125 is a key step for the CO_2-dependent opening of the Cx26 hemichannel. Mutation of this residue to Arg ($Cx26^{K125R}$), completely removes the CO_2 sensitivity of Cx26 hemichannels (Meigh et al., 2013). This is because Arg is more basic than Lys and therefore cannot be carbamylated by CO_2. We found that gap junctions formed between $Cx26^{K125R}$ expressing HeLa cells were insensitive to CO_2 (Figure 4,5a; change in conductance 0.01 nS, 95% confidence limits 0.2 and -0.06 nS, n=14). We used transfer of NBDG to verify that the K125R mutation abolished the CO_2-dependent closing of Cx26. Our data showed that unlike wild type Cx26 gap junctions, CO_2 made no difference to the rate of dye transfer between cells coupled via $Cx26^{K125R}$ (Figure 5b). We next tested whether the mutation R104A, which also removes CO_2 sensitivity from Cx26 hemichannels (Meigh et al., 2013), affected the CO_2 sensitivity of Cx26 gap junctions. CO_2 made no difference to the rate of dye transfer between cells coupled via $Cx26^{R104A}$ (Figure 5b).

Our results therefore suggest two important conclusions. Firstly, the action of CO_2 in closing Cx26 gap junctions is a direct effect on the gap junction dodecamer, and not an indirect effect mediated via changes in intracellular pH. Secondly, the same residues and carbamate-bridging mechanism that triggers Cx26 hemichannels opening, also causes Cx26 gap junctions to close.

Elastic network modelling

Previous experimental data points to the importance of K125 and the formation of a salt bridge to R104 in the adjacent subunit in the role of CO_2 in maintaining the Cx26 hexameric hemichannel in the open state. It is not clear from this finding why the dodecameric Cx26 gap junction would be closed by CO_2. Previous work had used course-grained modelling to demonstrate a mechanism whereby CO_2 constrains the Cx26 hemichannel in the open state (Meigh et al., 2013). We therefore used further course-grained modelling to probe the difference in behaviour of the Cx26 hemichannel and gap junction. Course-grained modelling reduces protein atomistic complexity for efficient computational studies of harmonic protein dynamics and is particularly suited to examining channel opening over millisecond time scales (Sherwood et al., 2008). In an Elastic Network Model (ENM) the $C\alpha$-atom co-ordinates of an atomic resolution structure are used to represent a protein structure. Global protein harmonic motions within the ENM consists of a defined number of modes, each of a characteristic frequency and representing a particular harmonic motion within the protein. ENMs reproduce protein global low frequency modes well in comparison to experimental data (Delarue and Sanejouand, 2002; Valadie et al., 2003). We therefore built coarse-grained ENMs (Tirion, 1996) to gain insight into the mechanism by which CO_2 maintains the Cx26 hemichannel in the open state but the Cx26 gap junction in the closed state. ENMs were constructed using the co-ordinates from high-resolution crystal structures for the Cx26 hemichannel and gap junction in the CO_2 unbound state. CO_2 was represented in the ENMs by the inclusion of additional Hookean springs between residues K125 and R104 of neighbouring monomers in both the hemichannel and the gap junction (Meigh et al., 2013).

We examined the similarities between eigenvectors for the Cx26 hemichannel and gap junction to understand the changes in harmonic protein motion caused by CO_2-binding. The main open-close mode in the hemichannel in the absence of CO_2 (mode 7) becomes reordered as mode 15 in the presence of CO_2 (Figure 6A; red-bordered square). That is, the open-close motion, with a higher mode number, contributes less to the total motion in the CO_2-bound state. The main open-close mode in the gap junction in the absence of CO_2 (mode 10; modes 7-9 represent motions between the two hexamer rings) becomes reordered as mode 24 in the presence of CO_2 (Figure 6B; green-bordered square). These data demonstrate a change in the contribution of the open-close motion to total protein motion in the Cx26 hemichannel and gap junction. However, this does not distinguish whether the gap junction is constrained in the open state (similar to the hemichannel) or the closed state.

To understand the differing roles of CO_2 in the hemichannel and gap junction, we calculated a range of partially open and closed eigenvectors for both the hemichannel and the gap junction. We then calculated at each state, for both the hemichannel and gap junction, the free energy for CO_2-binding

and the influence of CO_2 on the open/close eigenvector. This calculation provides a free energy for each state examined along the open/close eigenvector. Calculation of the free energy difference between the CO_2-bound and unbound state provides information on the stability (binding energy of CO_2 needed) for each state. In this case, the closer the value is to zero, the less energy needed to bind CO_2 (Figure 6C). The *x*-axis of the Figure represents trajectory along the open/close eigenvector where the higher the value the more closed the hemichannel or gap junction. The *y*-axis of the Figure represents the free energy for binding CO_2 where the higher the value the less preferable is CO_2-binding. On binding CO_2, the hemichannel or gap junction will progress along the open/close eigenvector to make the free energy of binding CO_2 energetically more favourable.

For the hemichannel, it is energetically favourable to bind CO_2 in the open-state and then energetically unfavourable to close. For the gap junction it is energetically favourable to bind CO_2 in the closed state and then energetically unfavourable to open. The differences in the open/closed state of the gap junction and hemichannel in response to CO_2 can therefore be explained through entropy contributions to free energy change.

Discussion

The key result from our study is that Cx26 gap junctions and hemichannels are modulated in opposite manners by CO_2. CO_2 closes the gap junction but opens the hemichannel. Yet CO_2 has these diametrically opposite actions on the two entities by interacting via the same residues, and therefore presumably through the same carbamate bridging mechanism.

Implications for structural biology of Cx26

The crystal structure of Cx26 shows the molecule in the form of a gap junction (Maeda et al., 2009). The two connexons dock via interactions involving the two extracellular loops (E1 and E2) of each subunit. There are multiple hydrogen bonds formed between the opposing E1 and E2 loops of each connexon (Maeda et al., 2009). These give a tight interaction that is likely to alter and constrain the conformation of hemichannels docked in a gap junction versus undocked hemichannels. The opposing modulation of gap junctions and hemichannels by CO_2 must presumably arise from the conformational differences between free versus docked hemichannels.

Our Elastic Network Modeling of the interaction of CO_2 with Cx26 hemichannels uses the docked hemichannel from the gap junction as a model for the structure of the free hemichannel (Meigh et al., 2013). This model allowed us to propose a plausible gating mechanism for CO_2-dependent opening of the hemichannel, which we have supported with extensive mutational analysis (Meigh et

al., 2013). We exploited this knowledge to introduce novel gating mechanisms via the same intersubunit interactions by mutating Lys125 to Cys (Meigh et al., 2015). This made the hemichannel NO-sensitive, via nitrosylation of the Cys125 and interaction with Arg104 of the neighbouring subunit. The double mutation -K125C, R104C - made the hemichannel redox sensitive (via redox modulation of disulfide bridges between subunits) (Meigh et al., 2015). The mutated residues in these Cx26 variants are some considerable distance apart –far further than the short distances normally required for the ionic and covalent interactions between the respective residues. That these mutations were nevertheless effective at changing the gating of Cx26 implies considerable flexibility of the hemichannel that can bring apparently distant residues close enough to interact (Meigh et al., 2015).

Despite this success in using a half gap junction as a model for the free hemichannel, the results in this study suggest the need for considerable caution in any future structural modeling of hemichannels. Not only may the isolated hemichannel be far more flexible than a hemichannel that is part of a gap junction, but it may also have a substantially different conformation. New structures of Cx26 hemichannels and gap junctions are therefore needed to probe their conformational differences, and provide firm mechanistic understanding of the differential modulation of hemichannels and gap junctions by CO_2.

Reversibility

The closure of the Cx26 gap junction appears to be less reversible than the opening of Cx26 hemichannels. There are 6 potential binding sites for CO_2 in the Cx26 hemichannel. The Hill coefficient for the effect of CO_2 on the hemichannel has been estimated between 4-6 (Huckstepp et al., 2010a; de Wolf et al., 2017), suggesting that several CO_2 molecules may be required to bind to open the hemichannel. For the complete gap junction there are 12 possible binding sites for CO_2. While we do not know how many molecules of CO_2 need to bind to close Cx26 gap junctions, or whether there might be cooperativity involved in CO_2 binding, it is possible that if all 12 binding sites were occupied, the resulting structure might be in a relatively stable closed configuration that would require significant time to reverse.

Physiological implications

As Cx26 exists both as gap junctions and hemichannels, our findings have substantial physiological significance. In the context of breathing, Cx26 hemichannels are important and we have already explored their significance for chemosensory control (Huckstepp et al., 2010b). However, there are reports of gap junctions in various nuclei implicated in the control of breathing (Dean et al., 2002;

Solomon et al., 2003). CO_2-dependent uncoupling of Cx26 gap junctions between cells may therefore be an additional mechanism that contributes to chemosensory control.

The supporting cells of the organ of corti in the cochlea have both functional Cx26 gap junctions and hemichannels: they are coupled by Cx26 gap junctions; and can also release ATP via Cx26 hemichannels (Zhao, 2005; Zhao and Yu, 2006; Majumder et al., 2010; Mammano, 2013; Zhu et al., 2013; Zhu et al., 2015). Cx26 gap junctions are a pathway for diffusion of K^+ between the fibrocytes, basal cells and intermediate cells of the stria vascularis (Wangemann, 2006) and have been proposed to form part of the pathway that recycles K^+ away from the hair cells, although this has been disputed (Zhao, 2017). Mutations of Cx26 are the commonest genetic cause of sensorineural hearing loss (Xu and Nicholson, 2013). Genetic deletion of Cx26 reduces the endocochlear potential by about half (Chen et al., 2014). Interestingly, the endolymph has a raised level of HCO_3^-, yet a pH of 7.5 indicating that PCO_2 of endolymph must be elevated (Wangemann, 2006). Furthermore, the stria vascularis, which creates the K^+ rich endolymph and the endocochlear potential essential for hearing, has a high energetic requirement (Marcus et al., 1978), and will thus be a strong local source of CO_2. We note that Cx30 and Cx31 gap junctions are also present in the cochlea (Wangemann, 2006). As Cx30 possesses the carbamylation motif, these gap junctions are likely to be CO_2-sensitive. Cx31 lacks the motif and these gap junctions are insensitive to CO_2 (Figure 4). It is therefore possible that some of the gap junction communication between the supporting cells and within the stria vascularis could be modulated by changes in PCO_2 and that this in turn could alter the sensitivity of hearing. However, this hypothesis would need to be directly tested.

More generally, we further speculate that if a single cell in a coupled network were to be excessively metabolically active, it would act as a sink for metabolites such as ATP, glucose or lactate from the coupled cells. As the metabolically active cell would produce more CO_2 this could be a self-regulating mechanism to dampen down that activity by uncoupling the cell from the network and reducing the supply of metabolites.

Methods

HeLa cell culture and transfection

HeLa Ohio (ECACC) cells were grown in EMEM supplemented with 1% non-essential amino acids, 10% fetal bovine serum, 50 µg/mL penicillin/streptomycin and 3 mM $CaCl_2$. For microscopy and dye loading experiments, cells were plated onto coverslips at a density of 1 x 10^5 cells per well of a 6-well plate. The cells were transiently transfected with Cx26 constructs containing a fluorescent marker, mCherry (1 µg) as described in the GeneJuice Transfection Reagent protocol (Merck Millipore).

Solutions used

Standard aCSF: 124 mM NaCl, 3 mM KCl, 2 mM $CaCl_2$, 26 mM $NaHCO_3$, 1.25 mM NaH_2PO_4, 1 mM $MgSO_4$, 10 mM D-glucose saturated with 95% O_2/5% CO_2, pH 7.5, PCO_2 35 mmHg.

Hypercapnic aCSF: 100 mM NaCl, 3 mM KCl, 2 mM $CaCl_2$, 50 mM $NaHCO_3$, 1.25 mM NaH_2PO_4, 1 mM $MgSO_4$, 10 mM D-glucose, saturated with 9% CO_2 (with the balance being O_2) to give a pH of 7.5 and a PCO_2 of 55 mmHg respectively.

Patch Clamp recordings

Cover slips containing non-confluent cells were placed into a perfusion chamber at room temperature in sterile filtered standard aCSF. Standard patch clamp techniques were used to make whole-cell recordings from either single HeLa cells or pairs of HeLa cells. The intracellular fluid in the patch pipettes contained: K-gluconate 120 mM, CsCl 10 mM, TEACl 10 mM, EGTA 10 mM, ATP 3 mM, $MgCl_2$ 1 mM, $CaCl_2$ 1 mM, sterile filtered, pH adjusted to 7.2 with KOH. All whole-cell recordings were performed at a holding potential of -50 mV with regular steps of 5 s to -50 mV to assess whole-cell conductance.

Cx26 mutants

The mutations used in this study were introduced into the Cx26 gene via the QuikChange method and have been described previously (Meigh et al., 2013).

Imaging assay of gap junction transfer

2-Deoxy-2-[(7-nitro-2,1,3-benzoxadiazol-4-yl)amino]-D-glucose, NBDG, was included at 200 μM in the patch recording fluid which was either the same as above or had lowered EGTA concentration (5mM). Cells were imaged on a Cleverscope (MCI Neuroscience) with a Photometrics Prime camera under the control of Micromanager 1.4 software. LED illumination (Cairn Research) and an image splitter (Optosplit, Cairn Research) allowed simultaneous imaging of the mCherry tagged Cx26 subunits and the diffusion of the NBDG into and between cells. Following breakthrough of the patch pipette to establish the whole cell mode, images were collected every 10 seconds.

Elastic network modelling

Elastic network model (ENM) simulations were performed based on the regular implementation using PDB file 2ZW3, where all the Cα atoms in the protein within a given cut-off radius (8 Å) were joined with simple Hookean springs (Tirion, 1996; Rodgers et al., 2013a). The spring constants were set to a constant value of 1 kcal mol^{-1} $Å^{-2}$. The presence of CO_2 was represented in the ENM by the

inclusion of an additional Hookean spring between residues K125 and R104 of each set of neighbouring monomers, following the same procedure previously used for ligand binding (Rodgers et al., 2013b). The mass-weighted second derivatives of this potential energy matrix were diagonalised to produce eigenvectors, *e*, which are the normal modes, and eigenvalues which are the squares of the associated frequencies, ω, and can be used to calculate the free energy of each mode.

The first six modes, that is the lowest frequency modes, represent the solid body translational and rotational motions of the protein and are thus ignored from the analysis. The overlap of the modes in the unbound and CO_2 bound states were calculated by comparison of the eigenvectors (Rodgers et al., 2013a). A value of 1 indicates that the motions are identical whereas a value of 0 indicates that the motions are completely different.

Statistical analysis

Statistical analysis was performed with the R language. Data has been plotted as box and whisker plots, with individual points superimposed, where the box is interquartile rage, bar is median, and whisker extends to most extreme data point that is no more than 1.5 times the interquartile range.

Acknowledgements

We thank the MRC (MR/P010393/1) for support. ND is a Royal Society Wolfson Research Merit Award Holder.

Author contributions

DM, SN, ND: Patch clamping, data collection and analysis

LM, EdW: Generation of mutants and stable cell lines

TR, MC: Elastic network modelling

ND wrote the paper, all authors commented on the final version.

Conflict of Interest Statement

The authors declare that they have no conflicts of interest.

References

Chen J, Chen J, Zhu Y, Liang C, Zhao HB (2014) Deafness induced by Connexin 26 (GJB2) deficiency is not determined by endocochlear potential (EP) reduction but is associated with cochlear developmental disorders. Biochem Biophys Res Commun 448:28-32.

de Wolf E, Cook J, Dale N (2017) Evolutionary adaptation of the sensitivity of connexin26 hemichannels to CO2. Proc Biol Sci 284.

Dean JB, Ballantyne D, Cardone DL, Erlichman JS, Solomon IC (2002) Role of gap junctions in CO(2) chemoreception and respiratory control. Am J Physiol Lung Cell Mol Physiol 283:L665-670.

Delarue M, Sanejouand YH (2002) Simplified normal mode analysis of conformational transitions in DNA-dependent polymerases: the elastic network model. J Mol Biol 320:1011-1024.

Huckstepp RT, Dale N (2011) Redefining the components of central CO2 chemosensitivity--towards a better understanding of mechanism. J Physiol 589:5561-5579.

Huckstepp RT, Eason R, Sachdev A, Dale N (2010a) CO2-dependent opening of connexin 26 and related beta connexins. J Physiol 588:3921-3931.

Huckstepp RT, id Bihi R, Eason R, Spyer KM, Dicke N, Willecke K, Marina N, Gourine AV, Dale N (2010b) Connexin hemichannel-mediated CO2-dependent release of ATP in the medulla oblongata contributes to central respiratory chemosensitivity. J Physiol 588:3901-3920.

Kang J, Kang N, Lovatt D, Torres A, Zhao Z, Lin J, Nedergaard M (2008) Connexin 43 hemichannels are permeable to ATP. J Neurosci 28:4702-4711.

Maeda S, Nakagawa S, Suga M, Yamashita E, Oshima A, Fujiyoshi Y, Tsukihara T (2009) Structure of the connexin 26 gap junction channel at 3.5 A resolution. Nature 458:597-602.

Majumder P, Crispino G, Rodriguez L, Ciubotaru CD, Anselmi F, Piazza V, Bortolozzi M, Mammano F (2010) ATP-mediated cell-cell signaling in the organ of Corti: the role of connexin channels. Purinergic Signal 6:167-187.

Mammano F (2013) ATP-dependent intercellular Ca2+ signaling in the developing cochlea: facts, fantasies and perspectives. Semin Cell Dev Biol 24:31-39.

Marcus DC, Thalmann R, Marcus NY (1978) Respiratory rate and ATP content of stria vascularis of guinea pig in vitro. The Laryngoscope 88:1825-1835.

Meigh L, Hussain N, Mulkey DK, Dale N (2014) Connexin26 hemichannels with a mutation that causes KID syndrome in humans lack sensitivity to CO2. Elife 3:e04249.

Meigh L, Cook D, Zhang J, Dale N (2015) Rational design of new NO and redox sensitivity into connexin26 hemichannels. Open Biol 5:140208.

Meigh L, Greenhalgh SA, Rodgers TL, Cann MJ, Roper DI, Dale N (2013) CO2 directly modulates connexin 26 by formation of carbamate bridges between subunits. Elife 2:e01213.

Pearson RA, Dale N, Llaudet E, Mobbs P (2005) ATP released via gap junction hemichannels from the pigment epithelium regulates neural retinal progenitor proliferation. Neuron 46:731-744.

Rodgers TL, Burnell D, Townsend PD, Pohl E, Cann MJ, Wilson MR, McLeish TC (2013a) ΔΔPT: a comprehensive toolbox for the analysis of protein motion. BMC Bioinformatics 14:183.

Rodgers TL, Townsend PD, Burnell D, Jones ML, Richards SA, McLeish TC, Pohl E, Wilson MR, Cann MJ (2013b) Modulation of Global Low-Frequency Motions Underlies Allosteric

Regulation: Demonstration in CRP/FNR Family Transcription Factors. PLoS Biol 11:e1001651.

Sherwood P, Brooks BR, Sansom MS (2008) Multiscale methods for macromolecular simulations. Current opinion in structural biology 18:630-640.

Solomon IC, Chon KH, Rodriguez MN (2003) Blockade of brain stem gap junctions increases phrenic burst frequency and reduces phrenic burst synchronisation in adult rat. Journal of Neurophysiology 89:135-149.

Stout C, Goodenough DA, Paul DL (2004) Connexins: functions without junctions. Curr Opin Cell Biol 16:507-512.

Stout CE, Costantin JL, Naus CC, Charles AC (2002) Intercellular calcium signaling in astrocytes via ATP release through connexin hemichannels. J Biol Chem 277:10482-10488.

Tirion MM (1996) Large Amplitude Elastic Motions in Proteins from a Single-Parameter, Atomic Analysis. Physical review letters 77:1905-1908.

Valadie H, Lacapcre JJ, Sanejouand YH, Etchebest C (2003) Dynamical properties of the MscL of Escherichia coli: a normal mode analysis. J Mol Biol 332:657-674.

Wangemann P (2006) Supporting sensory transduction: cochlear fluid homeostasis and the endocochlear potential. J Physiol 576:11-21.

Weissman TA, Riquelme PA, Ivic L, Flint AC, Kriegstein AR (2004) Calcium waves propagate through radial glial cells and modulate proliferation in the developing neocortex. Neuron 43:647-661.

Xu J, Nicholson BJ (2013) The role of connexins in ear and skin physiology - functional insights from disease-associated mutations. Biochim Biophys Acta 1828:167-178.

Zhao HB (2005) Connexin26 is responsible for anionic molecule permeability in the cochlea for intercellular signalling and metabolic communications. Eur J Neurosci 21:1859-1868.

Zhao HB (2017) Hypothesis of K(+)-Recycling Defect Is Not a Primary Deafness Mechanism for Cx26 (GJB2) Deficiency. Frontiers in molecular neuroscience 10:162.

Zhao HB, Yu N (2006) Distinct and gradient distributions of connexin26 and connexin30 in the cochlear sensory epithelium of guinea pigs. J Comp Neurol 499:506-518.

Zhu Y, Liang C, Chen J, Zong L, Chen GD, Zhao HB (2013) Active cochlear amplification is dependent on supporting cell gap junctions. Nat Commun 4:1786.

Zhu Y, Chen J, Liang C, Zong L, Chen J, Jones RO, Zhao HB (2015) Connexin26 (GJB2) deficiency reduces active cochlear amplification leading to late-onset hearing loss. Neuroscience 284:719-729.

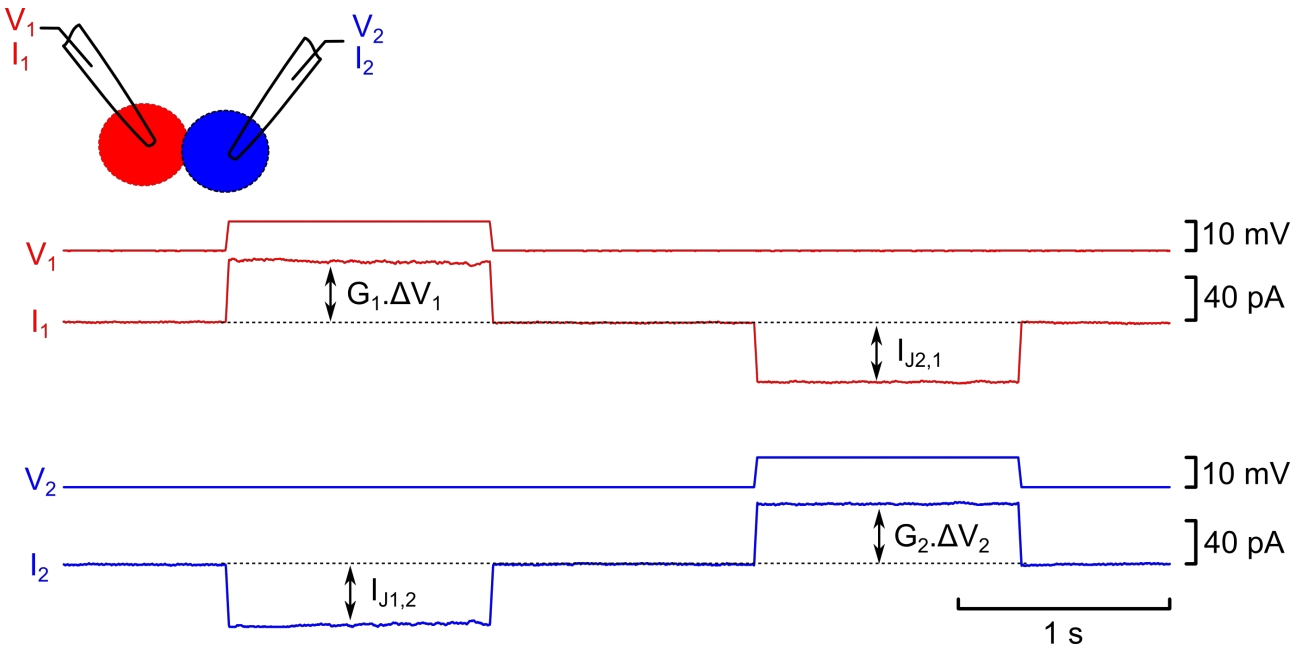

Figure 1. Voltage clamp protocol to measure simultaneously the whole cell conductance and junctional conductance in pairs of coupled HeLa cells. Both cells are clamped at -50 mV, and subjected to alternating 10 mV steps. $I_{J1,2}$ –current flow from cell 1 to cell 2; $I_{J2,1}$ –current flow from cell 2 to cell 1; G_1 –whole cell conductance of cell 1; G_2 –whole cell conductance of cell 2. Opening of Cx26 hemichannels will increase the whole cell conductance, whereas closure of Cx26 gap junctions will decrease $I_{J1,2}$ and $I_{J2,1}$ and decrease the whole cell conductance. The junctional conductance is simply $I_{J1,2}/(V_1-V_2)$ or $I_{J2,1}/(V_2-V_1)$. As Cx26 gap junctions display no rectification, both methods give the same value.

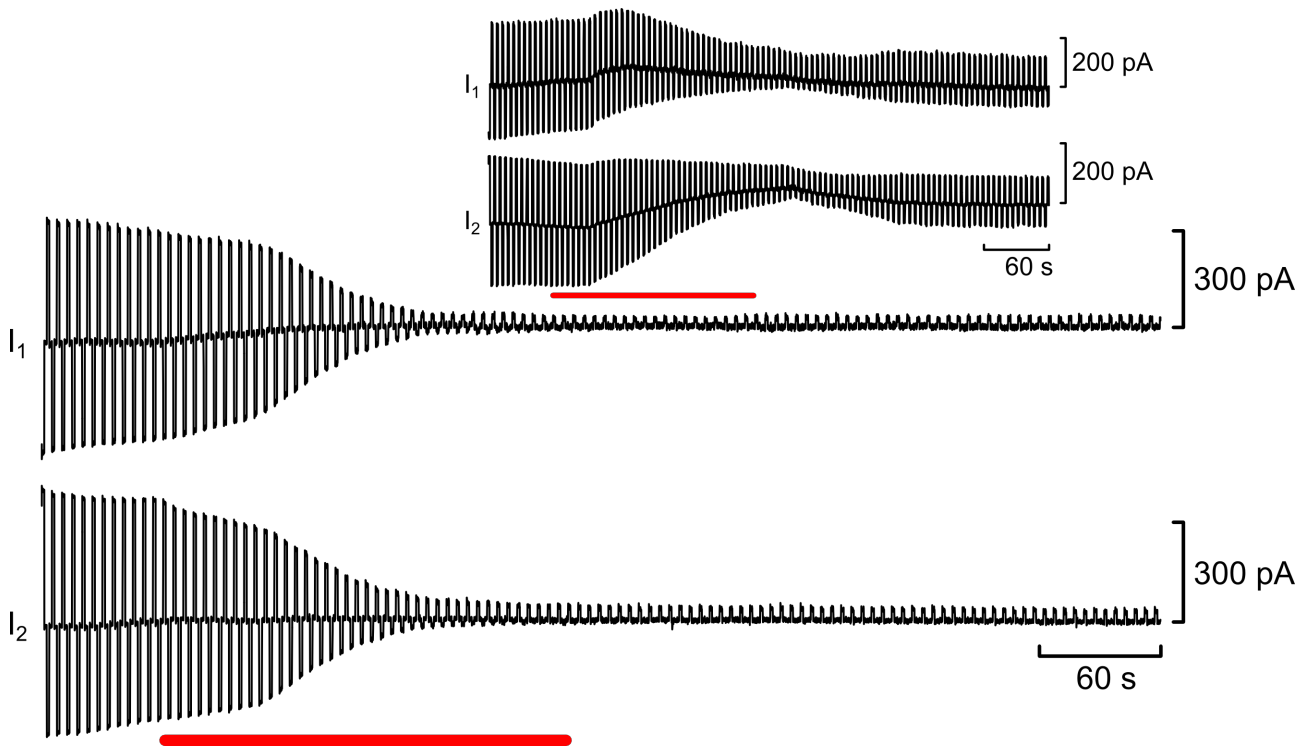

Figure 2. CO_2 closes Cx26 gap junctions. Main panel: hypercapnic saline (PCO_2 55 mmHg) applied at red bar, causes complete and irreversible closure of the gap junction. Note that the whole cell conductance also reduces (as a consequence of closure of the gap junction). Inset: example of a different pair of coupled cells, where there was partial closure of the gap junction in response to hypercapnic saline (red bar) that was at least partially reversible. The delay between the onset of gap junction modulation and application of hypercapnic saline results from the characteristics of the bath flow system.

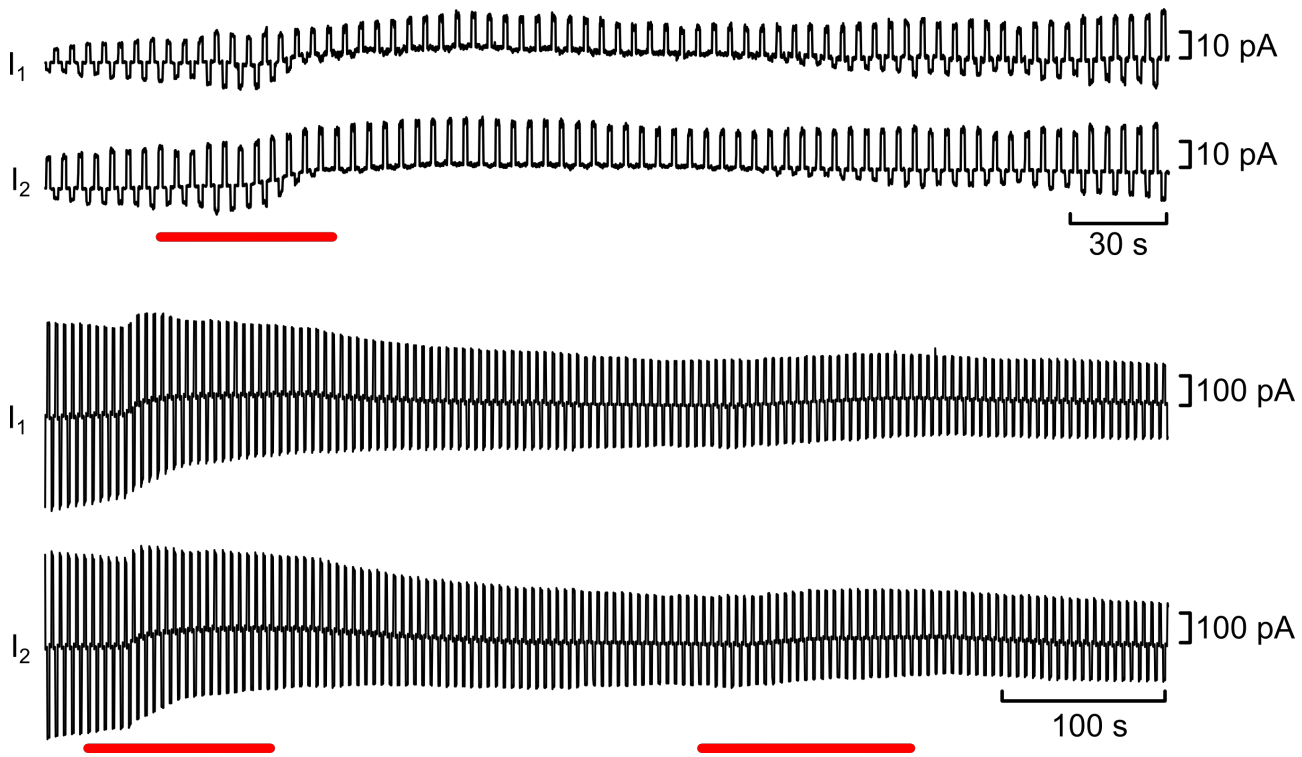

Figure 2, Supplement 1. The modulation of Cx26 gap junctions has variable reversibility. Top, an example of a gap junction that was completely blocked by hypercapnic saline (red bar), which also showed complete reversal of blockade on wash. Bottom, an example where there was partial block of the gap junction by hypercapnic saline (red bar), which did not reverse. Subsequent application of hypercapnic saline (red bar) had no further effect.

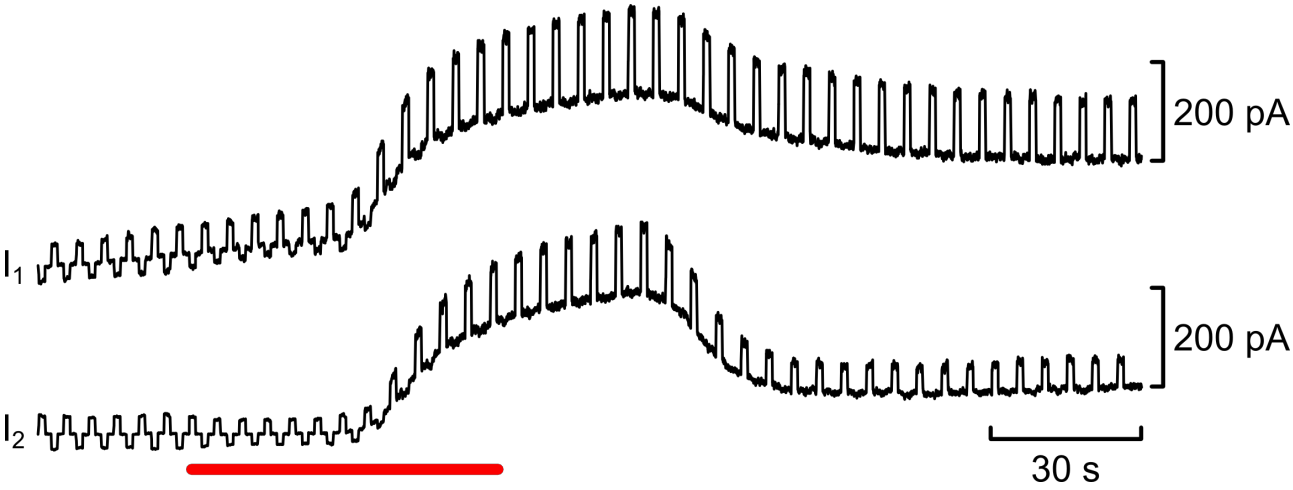

Figure 2, Supplement 2. Simultaneous modulation of Cx26 hemichannels and gap junctions in the same cells. When hypercapnic saline (red bar) was applied the whole cell conductance increased due to opening of the hemichannels (outward currents during voltage steps on each trace). However, at the same time the gap junction between the cells (inward currents during voltage steps) was blocked by CO_2. Note that the effect of CO_2 on the hemichannels reversed, but the blockade of the gap junction showed no reversal within the time course of the experiment.

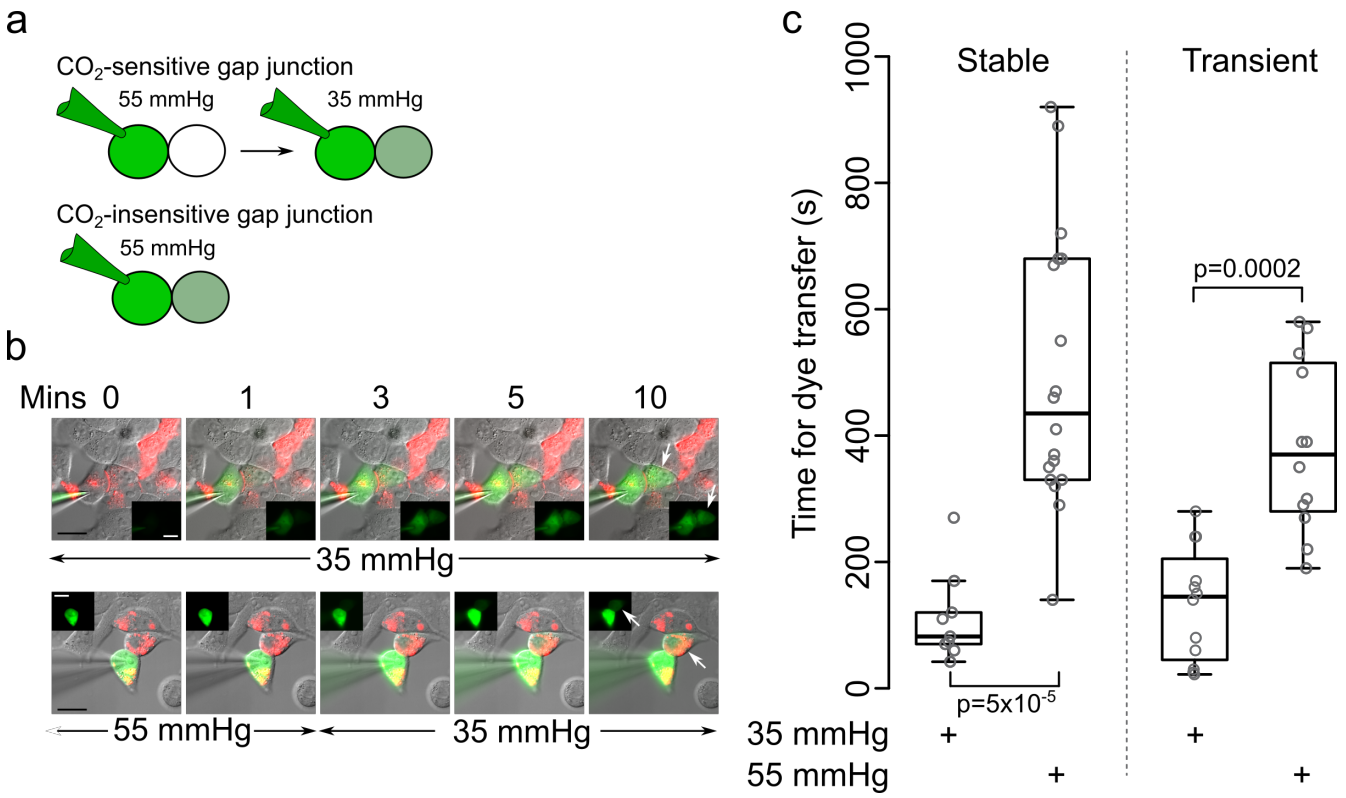

Figure 3. Dye transfer assay to assess the CO_2 sensitivity of gap junction coupling. a) Logic of the assay: a CO_2 sensitive gap junction will display no or very little dye transfer from the donor to acceptor cell under conditions of high PCO_2. This will occur once the cells are transferred to a low PCO_2 saline. A CO_2 insensitive gap junction will exhibit equally rapid dye transfer at low and high PCO_2. b) Images showing dye transfer between coupled cells. Montage of DIC and mCherry (for Cx26, red) and NBDG fluorescence (green). The gap junction can be observed as a red stripe between the coupled cells. Inset shows just the NBDG fluorescence. In 35 mmHg PCO_2 dye transfer to the acceptor cell is evident after 3 minutes (white arrows at 10 minutes). A PCO_2 of 55 mmHg greatly slows dye transfer and very little fluorescence in the acceptor cell is seen after 10 minutes (white arrow). c) Summary data for stably expressing (N=9 and 18 for low and high CO_2 respectively) and transiently transfected (N=12 for low and high CO_2) HeLa cells, showing the time for dye in the acceptor cell to reach 10% of the donor starting in 35 mmHg, and starting in 55 mmHg but transferring to 35mmHg after two minutes. When the recordings are commenced in 55 mmHg the dyes transfer time is much longer.

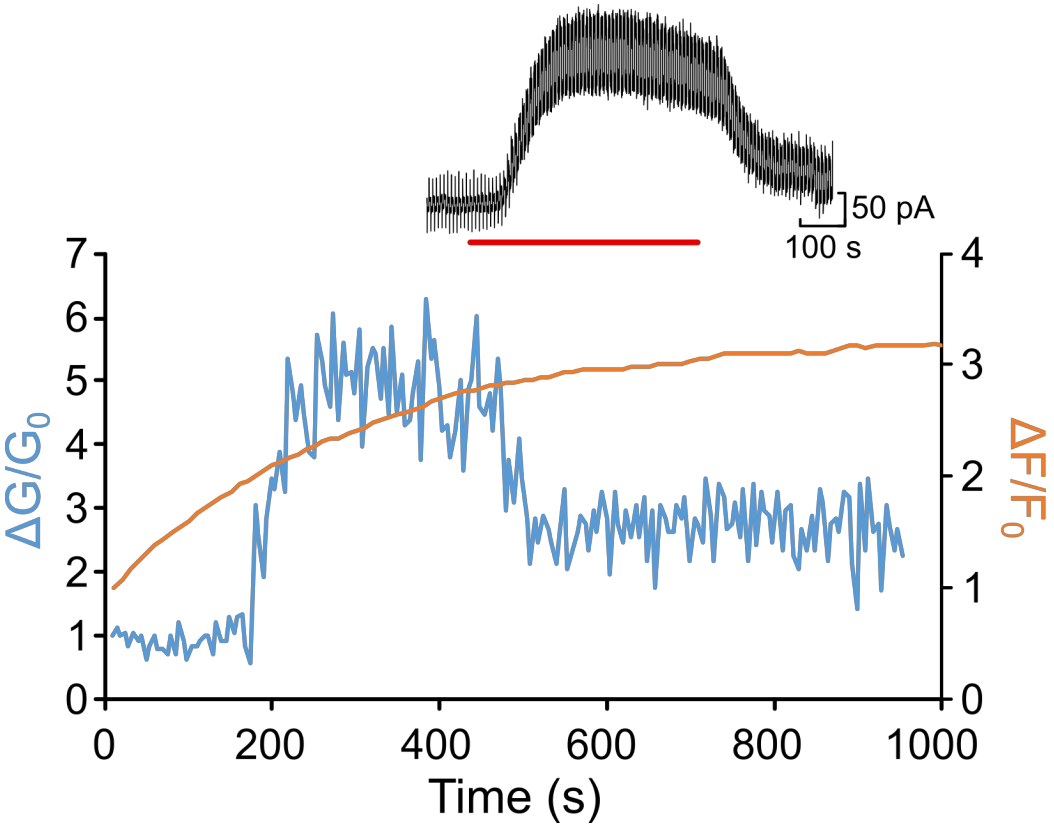

Figure 3 Supplement 1. **NBDG does not permeate Cx26 hemichannels.** Whole cell conductance and NBDG fluorescence changes for a single isolated Cx26-expressing cell exposed to CO_2. Inset, whole cell voltage clamp recording of HeLa cell transiently expressing Cx26, high CO_2 (PCO_2 55 mmHg) was applied at the red bar, and evoked a conductance change indicated by the increase in current flowing across the membrane during the regular 10 mV test steps. Main graph, comparison of the whole conductance changes in the cell and the changes in fluorescence. CO_2 evoked a reversible increase in whole cell conductance, but no loss of fluorescence was seen from the cell - instead there was continued loading of NBDG from the patch pipette into the cell. From 6 isolated cells the mean change in normalized NBDG fluorescence evoked by an increase in PCO_2 was 0.03 ± 0.045 (mean ± SD, n=6). NBDG therefore does not appear to permeate the Cx26 hemichannel as a fall in fluorescence would have been expected when the hemichannel opened (as indicated by the increase in whole cell conductance).

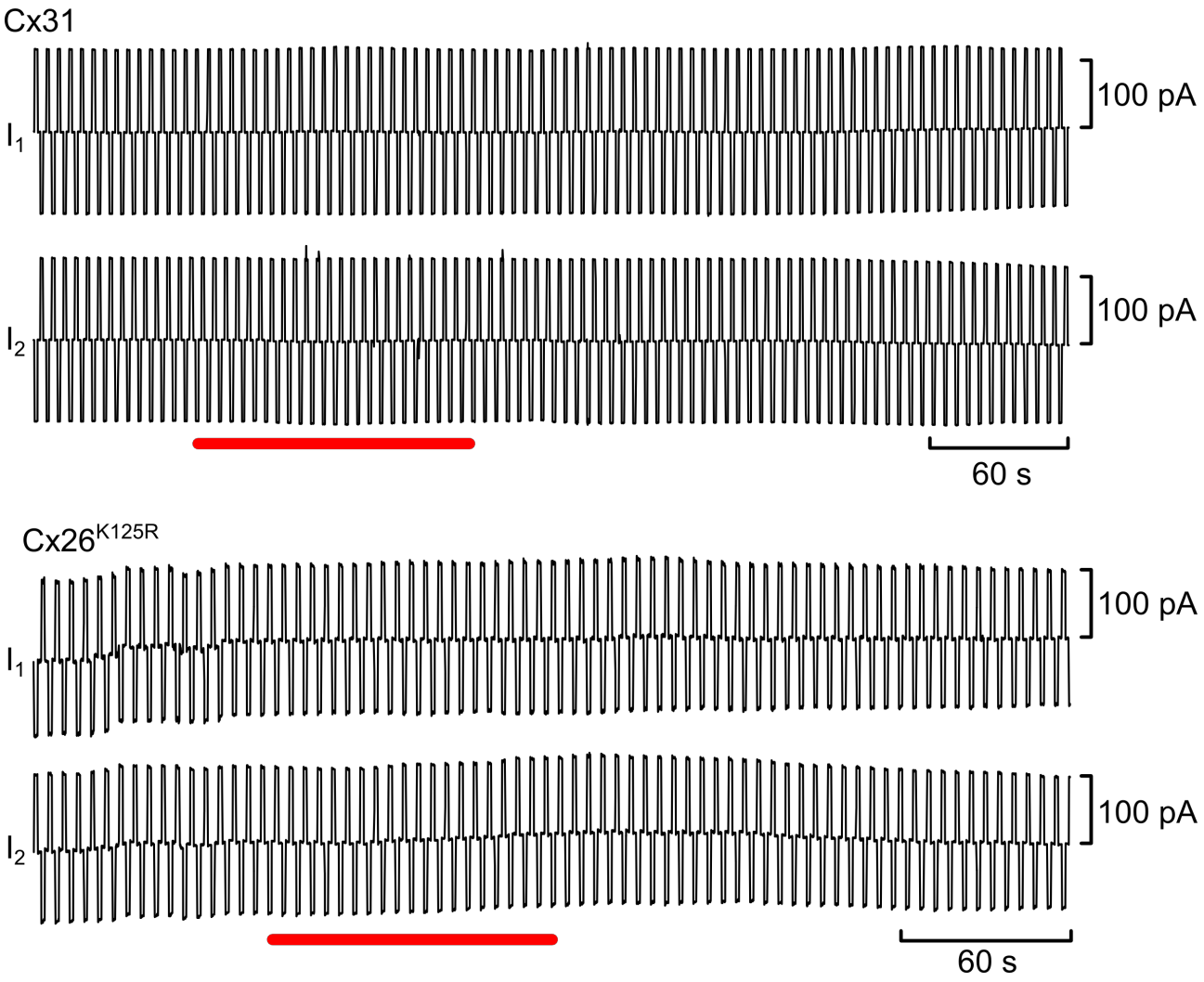

Figure 4. The CO_2 dependence of Cx26 gap junctions requires the carbamylation motif. Top) Cx31 gap junctions, which lack the carbamylation motif) are insensitive to CO_2. The mutation K125R which prevents carbamylation also removes CO_2 sensitivity of the gap junction.

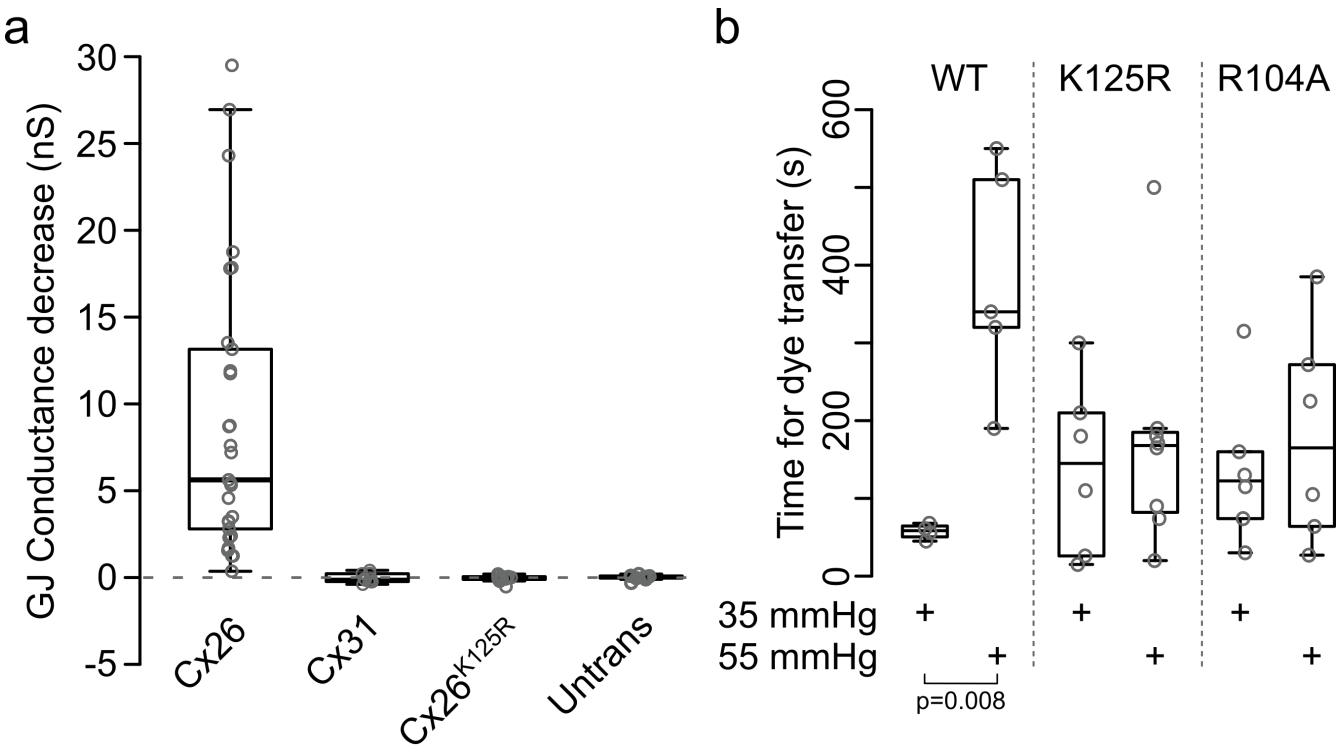

Figure 5. CO_2 dependence of Cx26 gap junction closing depends on the carbamylation motif. a) Gap junctions in HeLa cells Cx31 and $Cx26^{K125R}$ exhibit no CO_2-dependence. Gap junctions occasionally seen between parental HeLa cells (Untrans) display no CO_2-dependence either. Only WT Cx26 gap junctions exhibit a CO_2-dependent conductance decrease. b) Dye transfer assays show that WT Cx26 gap junctions are clearly CO_2 sensitive (55 mmHg PCO_2 delays the passage of dye across the gap junction), but those comprised of $Cx26^{K125R}$ or $Cx26^{R104A}$ show no CO_2-dependence in the time required for dye transfer from the donor to acceptor cell. Mann Whitney U test WT 35mmHg vs WT 55 mmHg, p=0.008.

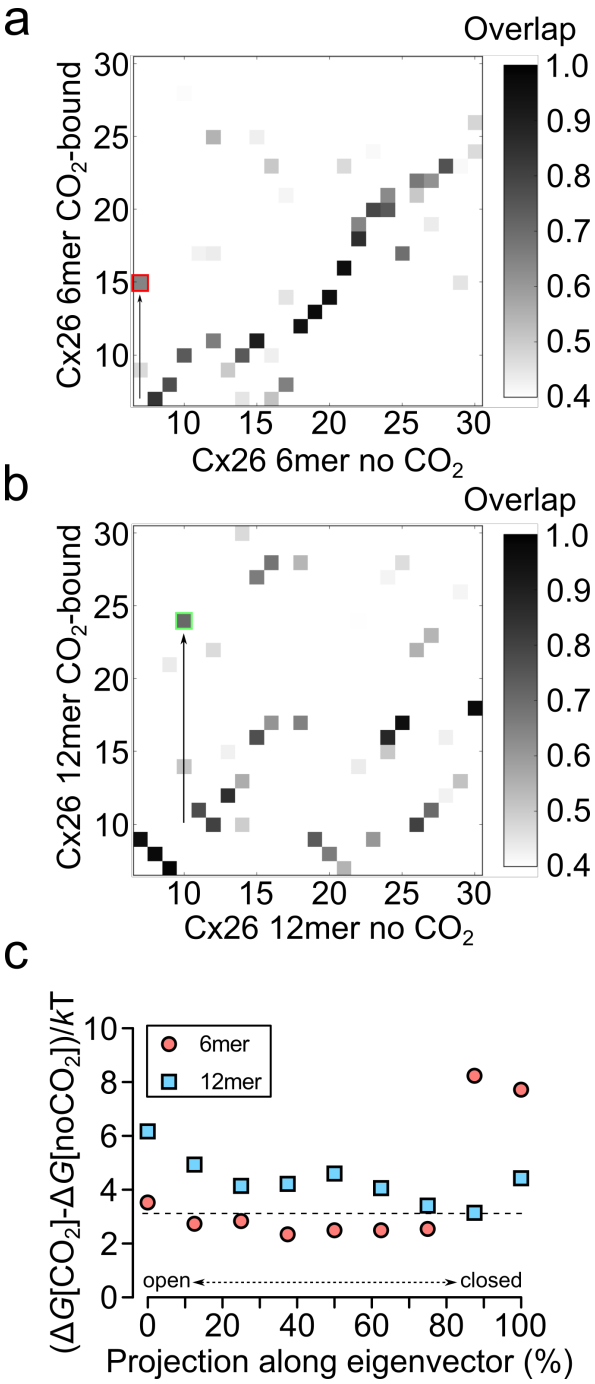

Figure 6. Analysis of the effect of CO_2 on Cx26 hemichannel and gap junction gating via elastic network modelling. a) The main open-close mode in the 6mer (hemichannel) in the absence of CO_2 (mode 7) is reordered to mode 15 (red square) in the presence of CO_2. Therefore, this mode contributes less to the total motion of the molecule in the presence of CO_2 -the hemichannel spends more time open (Meigh et al., 2013). b) The main open-close mode in the 12mer (gap junction) in the absence of CO_2 (mode 10) is reordered to mode 24 (green square) in the presence of CO_2. CO_2 thus reduces the contribution of this mode to the total motion of the molecule, but it is not possible to state whether the gap junction is predominantly in the closed or open state from this analysis

alone. c) For a range of partially open and closed eigenvectors for both the 6mer and the 12mer, we then calculated the change in free energy on CO_2-binding and thus the influence of CO_2 on the open/closed eigenvector. The closer the free energy value is to zero, the less energy needed to bind CO_2. The *x*-axis represents trajectory along the open/closed eigenvector going from fully open to fully closed. The *y*-axis represents the free energy for binding CO_2 where the higher the value the less preferable is CO_2-binding. For the 6mer, CO_2-binding is less energetically favourable in the closed state, whereas for the 12mer CO_2-binding is favoured in the closed state.